



Huppert, H. E., Hinton, E., & Hogg, A. J. (2020). *Defending against lava flows: theory, experiments and field confirmation*. Paper presented at 3rd Conference of the Arabian Journal of Geosciences, Sousse, Tunisia.

Peer reviewed version

[Link to publication record in Explore Bristol Research](#)
PDF-document

University of Bristol - Explore Bristol Research

General rights

This document is made available in accordance with publisher policies. Please cite only the published version using the reference above. Full terms of use are available:
<http://www.bristol.ac.uk/red/research-policy/pure/user-guides/ebr-terms/>

32 2 The model

33 Consider a time independent two-dimensional flow of flux Q per unit width of thin, vis-
 34 cous, Newtonian liquid, of kinematic viscosity ν , to model a lava flow down an inclined
 35 plane at angle β to the horizontal. The thickness of the flow is then given by [4]

$$36 \quad H_\infty = (3\nu Q/g \sin \beta)^{\frac{1}{3}}. \quad (2.1)$$

37 To this (vertical) lengthscale can be added horizontal and vertical lengthscales L and D
 38 dependent on the topography or building on the slope encountered by the lava flow.
 39 Introducing downslope and cross-slope dimensionless variables x and y , and a dimen-
 40 sionless axis perpendicular to the slope z by

$$41 \quad (x, y) = (X, Y)/L, \quad z = Z/H_\infty, \quad (2.2)$$

42 we find that the dimensionless depth $h(x, y)$ of the lava satisfies [1]

$$43 \quad (\partial h^3)/\partial x = \nabla[h^3 \nabla(\mathcal{F}(h + \mathcal{M}m))], \quad (2.3)$$

44 where $m(x, y)$ is a dimensionless expression for the underlying topography, along with
 45 the governing non-dimensional parameters

$$46 \quad \mathcal{F} = H_\infty/L \tan \beta = (3\nu Q/g \sin \beta)^{1/3}/(L \tan \beta). \quad (2.4)$$

$$47 \quad \text{and} \quad \mathcal{M} = D/L \tan \beta. \quad (2.5)$$

48 3 Flow patterns

49 3.1 One-dimensional mounds

50 Consider, to start and to illustrate some of the fundamental aspects of the flows, a one-
 51 dimensional situation (independent of the cross-flows co-ordinate, y), with the mound
 52 given by $m(x)$. (2.3) can then be integrated once, using the boundary condition $h \rightarrow 1$
 53 as $x \rightarrow -\infty$, to obtain

$$54 \quad h^3(1 - \mathcal{M} \frac{dm}{dx}) = 1 + \mathcal{F}h^3 \frac{dh}{dx}. \quad (3.1)$$

55 Because it is one-dimensional, all the flow must go over the mound. The most important
 56 consequence, determined from numerical solution of (3.1) for a variety of $m(x)$, \mathcal{F} and
 57 \mathcal{M} is that for small \mathcal{M} , $\mathcal{M} < \mathcal{M}_c$, where \mathcal{M}_c is a critical value, dependent on the details
 58 of $m(x)$ and the value of \mathcal{F} , the flow progresses uniformly over the mound, with a down-
 59 ward sloping upper surface everywhere. However, for $\mathcal{M} > \mathcal{M}_c$ a pond develops up-
 60 stream of the obstacle, the surface of which is horizontal. The value \mathcal{M}_c is the smallest
 61 value of \mathcal{M} so that $1 - \mathcal{M}m'(x)$ is somewhere negative. As an example, for $m =$
 62 $\exp(-x^2)$, $\mathcal{M}_c = (e/2)^{1/2} \approx 1.16$.

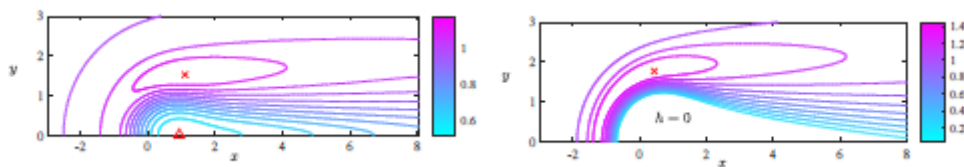
63

64 **3.2 Two-dimensional mounds**

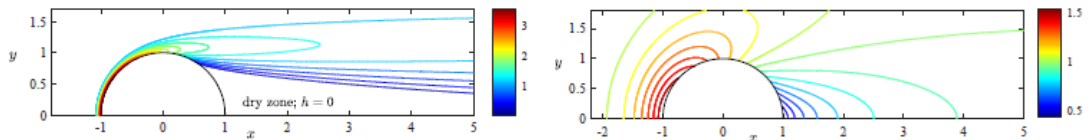
65 For mounds described by $m(x, y)$, the flow can: go over the mound; around the mound;
 66 not reach the top of the mound (if higher than some critical value); not completely cover
 67 the ground, that is, develop ‘dry patches’ - relatively safe places to be during a lava flow.
 68 Figure 1-4 display numerically determined flow fields for a variety of \mathcal{F} , \mathcal{M} and $m(x, y)$.
 69 An interesting series of examples is provided by an elliptical mound given by

70
$$m(x, y) = \exp\{-[x^2 + (y/b)^2]\}, \quad (3.2)$$

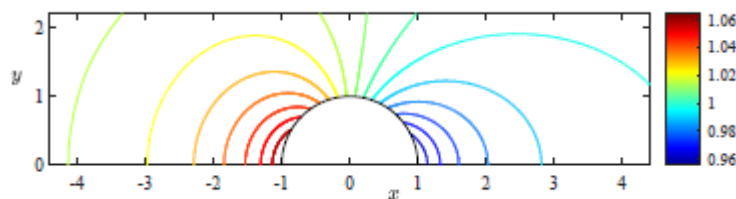
71 which tends to a long barrier as $b \rightarrow \infty$. Figure 5 shows the expected flow thickness for
 72 two values of b . What is the force exerted on such a topographic feature, envisaged as a
 73 defending wall to an oncoming lava flow? In the limit $b \rightarrow \infty$, for a barrier just suffi-
 74 ciently high to stop the oncoming flow (which climbs up the barrier) the maximum force
 75 $\sim \rho g (L \tan \beta)^2$, which for the illustrative values $L = 50m$ and $\tan \beta = 0.25$, leads to a
 76 maximum force of the order $10^7 Nm^{-1}$.
 77



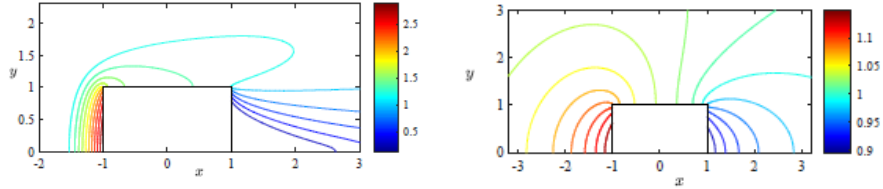
78
 79 Figure 1: Contour plots of the thickness of flow over topography specified by $m =$
 80 $\exp(-r^2)$ for $\mathcal{F} = 0.1$. a) $\mathcal{M} = 0.5$ and b) $\mathcal{M} = 1.5$. Red crosses mark the points of
 81 maximum thickness. Note the dry zone in b)



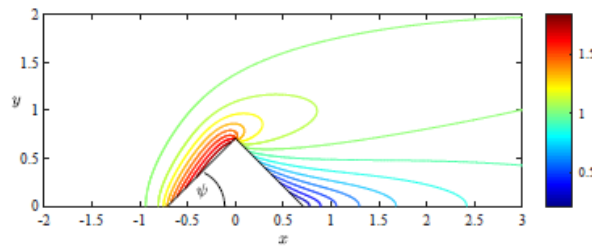
82



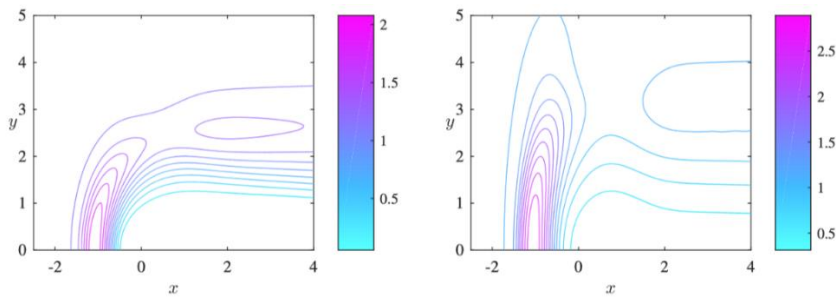
83
 84 Figure 2: Contour plots of the thickness of flow past a circular cylinder under the
 85 condition of no normal flow at the boundary, for $\mathcal{F} = 20, 1$ and 0.025 .
 86



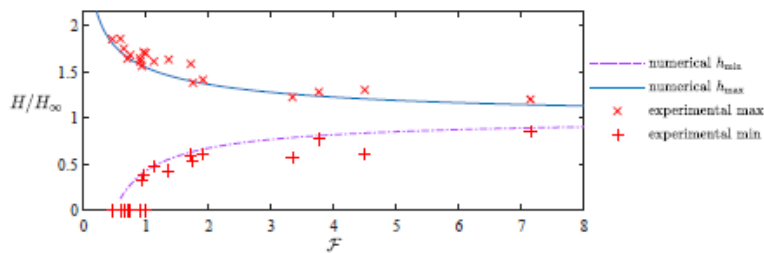
87
88 Figure 3: Contour plots of the thickness of flow around a square-on square obstacle for
89 $\mathcal{F} = 10$ and 0.25 . Note that the flow remains attached to the square in both cases and
90 there is no dry region for these values of \mathcal{F} .
91



92
93 Figure 4: Contour plot of the thickness of flow around a square rotated 45° to the
94 oncoming flow for $\mathcal{F} = 0.25$.
95



96
97 Figure 5: Contour plots of the thickness of flow over an elliptical mound with $\mathcal{F} = 0.05$
98 and $\mathcal{M} = 1.4$ for a) $b = 0.2$ and b) $b = 4$.



99
100 Figure 6: Calculated and experimental results for the maximum and minimum flow
101 thickness as a function of \mathcal{F} for flow past a cylinder. A zero flow thickness indicates the
102 existence of a dry zone downstream of the cylinder.

103

104 **3.3 Experimental verification**

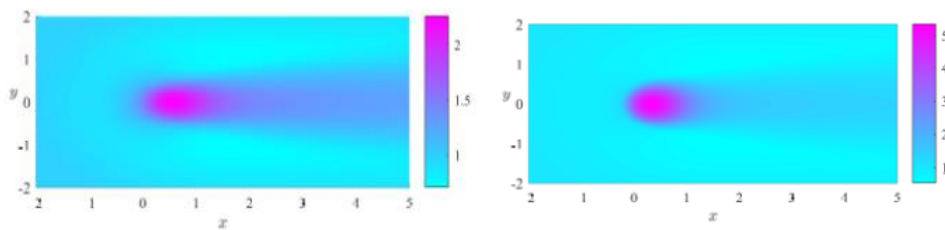
105 We carried out a series of experiments on a slope of width 30cm, length 120cm inclined
 106 at angles between 3.5 and 23 degrees on which we affixed (tall) cylinders of radius be-
 107 tween 2.4 and 4.8cm [2]. The upstream flow thickness varied between 0.5 and 1.5cm,
 108 leading to values of \mathcal{F} between 0.5 and 7.1 (the cylinders were all tall and so \mathcal{M} is not a
 109 relevant parameter.) Figure 6 displays a compendium of the results for the maximum
 110 and minimum flow thickness, with good agreement between theoretical predictions, ob-
 111 tained by numerically solving (2.3), and the experimental results.

112

113 **3.4 Depressions**

114 Real topography includes not only mounds and hills, but also depressions; and both
 115 together. An initial analysis of some effects due solely to depressions is contained in [3]
 116 and the flow thickness for two cases make up figure 7. For smallish depressions the flow
 117 thickness is but slightly perturbed. For deeper depressions large ponds of fluid accumu-
 118 late and have a significant effect on the flow downstream.

119



120

121 Figure 7: Flow thickness over a circular Gaussian depression for $\mathcal{F} = 0.1$ and a) $\mathcal{M} =$
 122 -0.8 and b) $\mathcal{M} = -1.6$.

123

124 Depressions are significantly different from hills because a sufficiently high hill, not
 125 touched by the flow at its higher points, does not come into contact with the flow; and
 126 hence the higher parts of the hill don't influence the flow. No matter how deep the de-
 127 pression it will influence the flow and there will be some flow (though maybe small)
 128 right to the bottom. In principle this resembles the influence of Moffatt eddies, slow
 129 motions in a sharp corner, well away from the forcing flow [5].

130

131 Of considerable interest and novelty are flows over topography containing both hills
 132 and depressions. We plan to publish on this topic in the future.

133

134 **3.5 Field observations**

135 Here is not the best place to compare our model results with real data taken in the
 136 field. However, numerous opportunities present themselves as outlined on Hawaii [6],
 137 Santorini [7] and elsewhere. This, too, will be reported elsewhere (Hinton et al. 2022).

138

139 **4 Conclusions**

140 Lava flows are frequent on the Earth and can cause much damage. Defending people
141 and property in such situations is a very worthwhile endeavor. Our work has begun to
142 lay down some of the foundations and principles that might be employed. Many further
143 questions remain, including what shape of cross-sectional area A (of a building) maxim-
144 ises the area of the dry zone. How sensitive is the result to the input parameters? How
145 will the concepts we have developed be used in any way usefully during forthcoming
146 volcanic eruptions?

147 **References**

- 148 1. Hinton, E.M., Hogg, A.J. and Huppert, H.E. Interaction of viscous free-surface flows with
149 topography. *Journal of Fluid Mechanics*, **876**, 912-938 (2019).
- 150 2. Hinton, E.M., Hogg, A.J. and Huppert, H.E. Viscous free-surface flows past cylinders. *Phys-*
151 *ical Review Fluids*, **5**, 1-30 (2020).
- 152 3. Hinton, E.M., Hogg, A.J. and Huppert, H.E. Free-surface viscous flows over a depression.
153 22nd Australasian Fluid Mechanics Conference AFMC 2020 (2020).
- 154 4. Lister, J.R. Viscous flows down an inclined plane from point and line sources. *Journal of*
155 *Fluid Mechanics*, 242, 631-653. (1992)
- 156 5. Moffatt, H.K. Viscous and resistive eddies near a sharp corner. *Journal of Fluid Mechanics*,
157 **18**, 1-18. (1964)
- 158 6. Neal, A.C. et al. The 2018 rift eruption and summit collapse of Kilauea Volcano. *Science*
159 **363**, 367-374 (2019).
- 160 7. Druitt, T.H., Edwards, L., Mellors, R.M., Pyle, D.M., Sparks, R.S.J., Lanphere M., Davies
161 M. and Barreiro B. Santorini volcano. *Geological Society Memoir* 19 (1999).
- 162